Published in final edited form as:
J Neurooncol. 2014 February ; 116(3): 543–549. doi:10.1007/s11060-013-1318-9.

Effect of contrast leakage on the detection of abnormal brain tumor vasculature in high-grade glioma

Peter S. LaViolette[#],
Department of Radiology, Medical College of Wisconsin, 8701 Watertown Plank Road, Milwaukee, WI 53226, USA

Mitchell K. Daun[#],
Department of Radiology, Medical College of Wisconsin, 8701 Watertown Plank Road, Milwaukee, WI 53226, USA

Eric S. Paulson, and
Department of Radiation Oncology, Medical College of Wisconsin, Milwaukee, WI, USA

Kathleen M. Schmainda
Department of Radiology, Medical College of Wisconsin, 8701 Watertown Plank Road, Milwaukee, WI 53226, USA; Department of Biophysics, Medical College of Wisconsin, Milwaukee, WI, USA

[#] These authors contributed equally to this work.

Abstract

Abnormal brain tumor vasculature has recently been highlighted by a dynamic susceptibility contrast (DSC) MRI processing technique. The technique uses independent component analysis (ICA) to separate arterial and venous perfusion. The overlap of the two, i.e. arterio-venous overlap or AVOL, preferentially occurs in brain tumors and predicts response to anti-angiogenic therapy. The effects of contrast agent leakage on the AVOL biomarker have yet to be established. DSC was acquired during two separate contrast boluses in ten patients undergoing clinical imaging for brain tumor diagnosis. Three components were modeled with ICA, which included the arterial and venous components. The percentage of each component as well as a third component were determined within contrast enhancing tumor and compared. AVOL within enhancing tumor was also compared between doses. The percentage of enhancing tumor classified as not arterial or venous and instead into a third component with contrast agent leakage apparent in the time-series was significantly greater for the first contrast dose compared to the second. The amount of AVOL detected within enhancing tumor was also significantly greater with the second dose compared to the first. Contrast leakage results in large signal variance classified as a separate component by the ICA algorithm. The use of a second dose mitigates the effect and allows measurement of AVOL within enhancement.

plaviole@mcw.edu.

Conflict of interest All authors report no conflict of interest.

Ethical standards This research was performed in approval of our institutional review board.

Keywords

Perfusion MRI; Independent Component Analysis (ICA); Dynamic Susceptibility Contrast (DSC); Brain Tumor; Glioblastoma

Introduction

High-grade gliomas are malignant brain tumors characterized by high infiltrative capacity and the ability to generate neoplastic vasculature. Termed angiogenesis, this development of new blood vessels is necessary to maintain high proliferation [1-5]. Brain tumor vascularity therefore provides not only a potential therapeutic target, but also a focus for qualitative and quantitative characterization with medical imaging.

Several MR perfusion imaging techniques have been developed to aid in the diagnosis of cerebrovascular disorders [6]. Dynamic susceptibility contrast MR (DSC-MR) imaging is dynamically gathered during the rapid bolus dose of contrast agent. DSC has gained clinical use because it identifies regions of abnormal tissue perfusion [7] and because it utilizes several quantitative measurements to characterize the brain's hemodynamics. In neuro-oncology, DSC-MRI provides preoperative insight into the histology of the neoplastic tissue [8], as well as distinguishes treatment effect such as radiation necrosis from true tumor recurrence [9-13].

A recent publication has demonstrated that areas classified by applying independent component analysis (ICA) to DSC data, as both arterial and venous (termed Arterio-Venous OverLap or AVOL) occur in greater proportion within tumor than normal tissue [14]. This study goes on to find that the change in the volume of AVOL within tumor predicted overall survival following treatment with the vascular endothelial growth factor (VEGF) inhibitor bevacizumab. Patients that showed an overall decrease in volume of AVOL had an increased median survival of 399 days versus 153 days for patients showing an increase in AVOL [14]. AVOL therefore appears to have potential as a non-invasive biomarker for characterizing tumor vascularity and evaluating treatment efficacy.

The AVOL biomarker is derived from ICA applied to DSC imaging. It is unclear, however, what effect contrast agent leakage has on the generation of AVOL maps, as normal intact vasculature lacks leakage. The previously published AVOL study used DSC data gathered during a second contrast agent dose [14]. Because collection of DSC data during a second bolus is not a universal practice, it is necessary to determine the effect of different contrast dosing techniques on the AVOL biomarker. This will provide evidence as to whether a second dose is requisite for AVOL calculation.

The purpose of this study was to determine the effect leakage has on the AVOL biomarker. We first hypothesized that during an initial dose, voxel time-series affected by contrast leakage would comprise an additional component (i.e. not arterial or venous). Second, we hypothesized that a greater percentage of voxels within enhancing tumor would be classified as AVOL following a reduction in leakage due to administration of a second dose.

Methods

Ten patients with high-grade, contrast-enhancing gliomas were enrolled following informed consent. Subject information including tumor grade and type can be found in Table 1. At the time of imaging, five of the ten study patients had yet to undergo surgical resection, three had undergone resection, and two had undergone tumor biopsy without resection.

Images were acquired on a 1.5T MRI scanner (GE, Waukesha, WI). The first dose of 0.1 mmol/kg (pre-load) dose of gadodiamide (Omniscan) contrast agent was administered as single shot gradient-echo (GE) echo-planar imaging was collected. Clinical post-contrast T1-weighted imaging was then obtained followed by a second bolus of 0.2 mmol/kg gadodiamide, during which DSC data was again gathered with the same acquisition parameters [15]. 13 slices of DSC data were acquired with the following parameters: 5 mm, skip 1.mm slice prescription, fat suppression, 90° flip angle, TE: 30 ms, TR: 1 s, field of view: 220 × 220 mm^2, matrix size: 128 × 128, and voxel size: 172 × 5 × 5 mm^3 [15]. A 90° flip angle was chosen to maximize the leakage susceptibility of the acquisition.

Pre-processing of the DSC data consisted of the removal of the first 4 time points and motion correction using MCFLIRT (FMRIB tool library). Data was then processed using probabilistic independent component analysis [16,17] as implemented in MELODIC (FMRIB tool library). Three components were extracted from the each dose's DSC acquisition. Arterial and venous components were manually identified based on the neuroanatomical land-marks involved [18], utilizing the T1+Contrast (T1+C) scan as a reference underlay. Two independent observers (MKD and PSL) manually classified components as arterial, venous [14], or the third component. If disagreement occurred, a consensus was reached on a case-by-case basis. One patient had a severe motion artifact that occurred during one of their scans. This artifact comprised enough signal variance that the ICA algorithm modeled it as one of the three components. Rather than misclassifying this component, ICA was rerun modeling 4 components to account for this large source of variance. This resulted motion free arterial, venous, and leakage components.

Following manual classification of the statistically thresholded component maps (mixture modeled, alternative hypothesis testing $p > 0.5$ vs. null [16]), custom developed in-house scripts utilizing AFNI software [19] (afni.nimh.nih.gov/afni) were employed to identify voxels with overlapping arterial and venous components (AVOL regions). Data from both doses was processed in this way. To compare AVOL maps from the first and second DSC acquisitions, contrast-enhancing tumor regions of interest (ROIs) were manually drawn on the T1+C images acquired in the same slice prescription as the DSC data. Non-enhancing areas within external tumor margins including resection cavities, necrotic cores, and biopsy sites, were excluded. The enhancing tumor regions of interest were then resampled to the DSC voxel resolution for proper AVOL comparison using a nearest neighbor interpolation. To address the first hypothesis, the percentage of enhancing tumor occupied by each individual independent component (arterial, venous, and leakage) was calculated and compared across the two time points using a paired *t* test. The percentage of AVOL within enhancing tumor for each dose was similarly tested to address the second hypothesis. A

Bonferroni correction for multiple comparisons established $p < 0.0125$ as the level of significance.

To visualize the temporal dynamics of the group DSC signals, the mean ΔR2* was calculated for each patient. The individual DSC sessions were temporally synched by aligning the TR with the largest temporal change (i.e. the initial jump in ΔR2*) within the arterial component.

To ensure the untreated GBMs within the heterogeneous patient population were not skewing the results, the percentage of enhancing tumor occupied by each individual independent component (arterial, venous, and leakage) was calculated and compared between the untreated GBM and all others using a *t* test. The percentage of AVOL within enhancement was also compared.

Results

Figure 1 demonstrates the average ΔR2* signal for each component across the two doses. The effect of leakage is clearly seen in the first dose, yet mitigated with the second dose, where signal is shown from a mask defined by the leakage component from the first dose. Figure 2 shows two representative patients and the spatial extent of each component as well as the respective overlapping voxels present in both doses. Figure 3 shows the percentage of tumor occupied by each of the three ICA components for each dose. As illustrated, the data supports our first hypothesis that the third or leakage-affected component is significantly more prevalent in tumor when comparing the first dose to the second dose ($p < 0.001$). This suggests that leakage alters the signal within enhancing voxels enough that the algorithm classifies a greater proportion in the first dose scan as an independent component.

Figure 4 shows AVOL as a percentage of enhancing tumor compared to dose. AVOL comprises a significantly greater percentage of enhancing tumor during the second dose versus the first ($p < 0.01$). The data supports our hypothesis that AVOL is significantly affected by the contrast leakage effect in the first dose acquisition compared with acquisition during a second contrast dose.

Comparison of the untreated GBMs to the other five tumors yielded insignificant comparisons ($p > 0.2$) except for the percentage of pre-load arterial component within enhancement. For this comparison the untreated GBMs showed greater percentage and a trend towards significance ($p = 0.073$).

Discussion

This study explored how leakage effects the application of ICA to DSC MRI in cases of high-grade brain cancer. Our study found that contrast leakage into tumor occurring during the initial dose of contrast agent generated a large enough source of variance that it altered the ICA component classification. This was quantified by measuring the percentage of enhancing tumor occupied by arterial, venous, and a third ICA component (leakage-affected). The percentage of enhancing tumor represented in the leakage component was significantly lower during the second dose compared to the first. In addition, the percentage

of venous contribution rose significantly with the second dose. This study also found that the contrast leakage effect significantly decreased the amount of enhancing tumor with overlapping arterial and venous components (AVOL). This study provides evidence that a second dose of contrast in DSC perfusion imaging is likely necessary for maximizing the percentage of enhancement classified as AVOL.

DSC derived rCBV has been shown to be correlated with tumor grade [20-22] and vascularity [23, 24], and is predictive of patient survival [25]. Leakage of contrast agent from the vasculature into tumor tissue during bolus injection confounds DSC derived rCBV [26]. The injection of a second contrast dose has been shown to greatly mitigate the leakage effect [15, 26, 27], though disagreement exists as to its necessity [28]. The varied number of post processing techniques also complicates this issue [15].

ICA is a technique that objectively separates major sources of variance in dynamically acquired MRI data. Following its first use in fMRI [29], ICA has shown promising utility in analyzing brain activity when applied to fMRI [30] and EEG data [31]. ICA has also been used to differentiate the major phases of cerebral perfusion and their corresponding vessels [14, 18, 32, 33]. Constraining the ICA algorithm to three components adequately segregates the arterial and venous component based on their tissue perfusion characteristics [14, 18]. The third component is, however, subject to variability and in this study has been dominated by contrast leakage.

One of the more interesting aspects of our study was that while the proportion of venous component in tumor was significantly increased following the use of a second dose, the same correction for contrast leakage did not lead to a significant increase in the arterial percentage in tumor. One possible explanation for this heterogeneity is that VEGF induces angiogenesis of “mother vessels” which stem from preexisting venules [34]. Since the first vessels involved in angiogenesis stem from the venous side of the circulation, it is reasonable to assume that these new vessels would exhibit venous characteristics, and therefore would preferentially segregate as venous component when analyzed with ICA. Without histological validation, however, we can only speculate.

Figure 2 shows the distribution of the arterial and venous components. It should be noted that the third component in each patient, especially in the first dose data, highlighted the tumor and the choroid plexus. This left all of the normal white matter (WM) unclassified in any component. This is likely explained by the greater percentage of microvasculature leading to a lower signal to noise ratio (SNR). Because the maps considered for this analysis were statistically thresholded, these voxels fell short, and therefore belonged to no component in particular. Modeling a greater number of components would presumably lead to a component specifically highlighting WM [32]. We chose to model three components because previous studies have shown maximal spatial repeatability of the arterial and venous components occurs when three are modeled [35, 36].

There are several limitations to this study. Though our limited sample size of ten patients proved to be sufficient for measuring statistical significance, future studies with larger, more homogeneous populations are warranted. The small number recruited also meant that data

could not be excluded if large motion artifacts were present. As mentioned in the methods section, one patient's motion resulted in a large artifact. This was corrected by including an additional component in the ICA to model the variance associated. Also, as is the case in most fMRI ICA analyses, there is an element of subjectivity involved in classifying ICA components as arterial or venous. We remedied this by having two independent observers classify the components, then compare. Any disagreements were identified and a consensus was reached on a case-by-case basis. Four of the 60 total components required a consensus.

Another confound to this analysis is the large patient population heterogeneity. Five of the ten patients were scanned prior to any intervention for GBM's later pathologically confirmed. Two patients had lower grade III tumors and surgically, three had undergone resection, and two had undergone tumor biopsy without resection. These patients were treated with radiation and undergoing temozolomide treatment at the time of scanning. To ensure these patients were not skewing the results, we ran an additional analysis comparing the percentages of vascular components present within enhancement, and AVOL for each dose to the other five pre-treatment GBMs. We found no statistical differences between the groups save for GBMs trending towards significantly greater percentage of pre-load arterial component within enhancement. This suggests that untreated GBMs contain greater proportions of arterial like vasculature versus grade III and treated tumors. More research is necessary to determine the tumor grade dependence of ICA-DSC metrics.

Having established that a second dose of contrast agent is needed to maximize percentage of AVOL, future research should further explore the utility of the biomarker. In order to identify the role that ICA has in MR perfusion studies, exploration should be made into the repeatability of ICA in its application to DSC data. If it is validated, additional research can further explore the applications of ICA to MR perfusion data in order to better characterize the cerebrovasculature in cancer and stroke patients as well as in healthy individuals.

In summary, we find that contrast leakage provides a significant source of variance in first contrast dose DSC data upon analysis with ICA. This variance occurs preferentially in the tumor margin due to the presence of "leakier" vasculature, causing ICA to model the majority of tumor as its own component. The variance caused by leakage effectively masks the vasculature within the tumor margin, and leads to an underestimation of venous ICA component and arterio-venous overlap (AVOL) inside tumor. Acquiring DSC data after administration of a second contrast dose significantly mitigates the contrast leakage effect, and results in a larger portion of AVOL within enhancing tumor.

Acknowledgments

Special thanks to the patients who chose to participate in this study. This work was funded by NIH/NCI R01CA082500, and Advancing a Healthier Wisconsin.

References

1. Louis DN, Ohgaki H, Wiestler OD, Cavenee WK, Burger PC, Jouvet A, Scheithauer BW, Kleihues P. The 2007 WHO classification of tumours of the central nervous system. Acta Neuropathol. 2007; 114:97–109. [PubMed: 17618441]

2. Deane BR, Lantos PL. The vasculature of experimental brain tumours. Part 1. A sequential light and electron microscope study of angiogenesis. J Neurol Sci. 1981; 49:55–66. [PubMed: 7205320]
3. Folkman J. What is the evidence that tumors are angiogenesis dependent? J Natl Cancer Inst. 1990; 82:4–6. [PubMed: 1688381]
4. Millauer B, Shawver LK, Plate KH, Risau W, Ullrich A. Glioblastoma growth inhibited in vivo by a dominant-negative Flk-1 mutant. Nature. 1994; 367:576–579. [PubMed: 8107827]
5. Leon SP, Folkerth RD, Black PM. Microvessel density is a prognostic indicator for patients with astroglial brain tumors. Cancer. 1996; 77:362–372. [PubMed: 8625246]
6. Lev MH, Rosen BR. Clinical applications of intracranial perfusion MR imaging. Neuroimaging Clin N Am. 1999; 9:309–331. [PubMed: 10318717]
7. Cha S, Lu S, Johnson G, Knopp EA. Dynamic susceptibility contrast MR imaging: correlation of signal intensity changes with cerebral blood volume measurements. J Magn Reson Imaging. 2000; 11:114–119. [PubMed: 10713942]
8. Covarrubias DJ, Rosen BR, Lev MH. Dynamic magnetic resonance perfusion imaging of brain tumors. Oncologist. 2004; 9:528–537. [PubMed: 15477637]
9. Gahramanov S, Raslan AM, Muldoon LL, Hamilton BE, Rooney WD, Varallyay CG, Njus JM, Haluska M, Neuwelt EA. Potential for differentiation of pseudoprogression from true tumor progression with dynamic susceptibility-weighted contrast-enhanced magnetic resonance imaging using ferumoxytol vs. gadoteridol: a pilot study. Int J Radiat Oncol Biol Phys. 2011; 79:514–523. [PubMed: 20395065]
10. Barajas RF Jr, Chang JS, Segal MR, Parsa AT, McDermott MW, Berger MS, Cha S. Differentiation of recurrent glioblastoma multiforme from radiation necrosis after external beam radiation therapy with dynamic susceptibility-weighted contrast-enhanced perfusion MR imaging. Radiology. 2009; 253:486–496. [PubMed: 19789240]
11. Hoefnagels FW, Lagerwaard FJ, Sanchez E, Haasbeek CJ, Knol DL, Slotman BJ, Vandertop WP. Radiological progression of cerebral metastases after radiosurgery: assessment of perfusion MRI for differentiating between necrosis and recurrence. J Neurol. 2009; 256:878–887. [PubMed: 19274425]
12. Hu LS, Baxter LC, Smith KA, Feuerstein BG, Karis JP, Eschbacher JM, Coons SW, Nakaji P, Yeh RF, Debbins J, Heiserman JE. Relative cerebral blood volume values to differentiate high-grade glioma recurrence from posttreatment radiation effect: direct correlation between image-guided tissue histopathology and localized dynamic susceptibility-weighted contrast-enhanced perfusion MR imaging measurements. AJNR Am J Neuroradiol. 2009; 30:552–558. [PubMed: 19056837]
13. Sugahara T, Korogi Y, Tomiguchi S, Shigematsu Y, Ikushima I, Kira T, Liang L, Ushio Y, Takahashi M. Posttherapeutic intraaxial brain tumor: the value of perfusion-sensitive contrast-enhanced MR imaging for differentiating tumor recurrence from nonneoplastic contrast-enhancing tissue. AJNR Am J Neuroradiol. 2000; 21:901–909. [PubMed: 10815666]
14. LaViolette PS, Cohen AD, Prah MA, Rand SD, Connelly J, Malkin MG, Mueller WM, Schmainda KM. Vascular change measured with independent component analysis of dynamic susceptibility contrast MRI predicts bevacizumab response in high-grade glioma. Neuro Oncol. 2013; 15:442–450. [PubMed: 23382287]
15. Paulson ES, Schmainda KM. Comparison of dynamic susceptibility-weighted contrast-enhanced MR methods: recommendations for measuring relative cerebral blood volume in brain tumors. Radiology. 2008; 249:601–613. [PubMed: 18780827]
16. Beckmann CF, Smith SM. Probabilistic independent component analysis for functional magnetic resonance imaging. IEEE Trans Med Imaging. 2004; 23:137–152. [PubMed: 14964560]
17. Hyvarinen A. Fast and robust fixed-point algorithms for independent component analysis. IEEE Trans Neural Netw. 1999; 10:626–634. [PubMed: 18252563]
18. LaViolette, PS.; Cohen, AD.; Schmainda, KM. Contrast leakage in high grade glioma measured with independent component analysis of dynamic susceptibility contrast MRI; Proc ISMRM; Melbourne. 2012;
19. Cox RW. AFNI: software for analysis and visualization of functional magnetic resonance neuroimages. Comput Biomed Res. 1996; 29:162–173. [PubMed: 8812068]

20. Law M, Yang S, Wang H, Babb JS, Johnson G, Cha S, Knopp EA, Zagzag D. Glioma grading: sensitivity, specificity, and predictive values of perfusion MR imaging and proton MR spectroscopic imaging compared with conventional MR imaging. AJNR Am J Neuroradiol. 2003; 24:1989–1998. [PubMed: 14625221]

21. Knopp EA, Cha S, Johnson G, Mazumdar A, Golfinos JG, Zagzag D, Miller DC, Kelly PJ, Kricheff II. Glial neoplasms: dynamic contrast-enhanced T2*-weighted MR imaging. Radiology. 1999; 211:791–798. [PubMed: 10352608]

22. Aronen HJ, Gazit IE, Louis DN, Buchbinder BR, Pardo FS, Weisskoff RM, Harsh GR, Cosgrove GR, Halpern EF, Hochberg FH, et al. Cerebral blood volume maps of gliomas: comparison with tumor grade and histologic findings. Radiology. 1994; 191:41–51. [PubMed: 8134596]

23. Sugahara T, Korogi Y, Shigematsu Y, Liang L, Yoshizumi K, Kitajima M, Takahashi M. Value of dynamic susceptibility contrast magnetic resonance imaging in the evaluation of intracranial tumors. Top Magn Reson Imaging. 1999; 10:114–124. [PubMed: 10551626]

24. Sugahara T, Korogi Y, Kochi M, Ikushima I, Hirai T, Okuda T, Shigematsu Y, Liang L, Ge Y, Ushio Y, Takahashi M. Correlation of MR imaging-determined cerebral blood volume maps with histologic and angiographic determination of vascularity of gliomas. AJR Am J Roentgenol. 1998; 171:1479–1486. [PubMed: 9843274]

25. Wong ET, Jackson EF, Hess KR, Schomer DF, Hazle JD, Kyritsis AP, Jaeckle KA, Yung WK, Levin VA, Leeds NE. Correlation between dynamic MRI and outcome in patients with malignant gliomas. Neurology. 1998; 50:777–781. [PubMed: 9521274]

26. Boxerman JL, Schmainda KM, Weisskoff RM. Relative cerebral blood volume maps corrected for contrast agent extravasation significantly correlate with glioma tumor grade, whereas uncorrected maps do not. AJNR Am J Neuroradiol. 2006; 27:859–867. [PubMed: 16611779]

27. Hu LS, Baxter LC, Pinnaduwage DS, Paine TL, Karis JP, Feuerstein BG, Schmainda KM, Dueck AC, Debbins J, Smith KA, Nakaji P, Eschbacher JM, Coons SW, Heiserman JE. Optimized preload leakage-correction methods to improve the diagnostic accuracy of dynamic susceptibility-weighted contrast-enhanced perfusion MR imaging in posttreatment gliomas. AJNR Am J Neuroradiol. 2010; 31:40–48. [PubMed: 19749223]

28. Spampinato MV, Wooten C, Dorlon M, Besenski N, Rumboldt Z. Comparison of first-pass and second-bolus dynamic susceptibility perfusion MRI in brain tumors. Neuroradiology. 2006; 48:867–874. [PubMed: 17013587]

29. McKeown MJ, Makeig S, Brown GG, Jung TP, Kindermann SS, Bell AJ, Sejnowski TJ. Analysis of fMRI data by blind separation into independent spatial components. Hum Brain Mapp. 1998; 6:160–188. [PubMed: 9673671]

30. Calhoun VD, Liu J, Adali T. A review of group ICA for fMRI data and ICA for joint inference of imaging, genetic, and ERP data. Neuroimage. 2009; 45:S163–S172. [PubMed: 19059344]

31. Onton J, Westerfield M, Townsend J, Makeig S. Imaging human EEG dynamics using independent component analysis. Neurosci Biobehav Rev. 2006; 30:808–822. [PubMed: 16904745]

32. Kao YH, Guo WY, Wu YT, Liu KC, Chai WY, Lin CY, Hwang YS. Jy-Kang Liou A, Wu HM, Cheng HC, Yeh TC, Hsieh JC, Mu Huo Teng M: Hemodynamic segmentation of MR brain perfusion images using independent component analysis, thresholding, and Bayesian estimation. Magn Reson Med. 2003; 49:885–894. [PubMed: 12704771]

33. LaViolette, PS.; Cohen, AD.; Rand, SD.; Mueller, WM.; Schmainda, KM. Independent component analysis of dynamic susceptibility contrast MRI in brain tumor: a new biomarker for measuring tumor perfusion patterns; Proc ISMRM; Montreal Quebec. 2011;

34. Senger DR, Van de Water L, Brown LF, Nagy JA, Yeo KT, Yeo TK, Berse B, Jackman RW, Dvorak AM, Dvorak HF. Vascular permeability factor (VPF, VEGF) in tumor biology. Cancer Metastasis Rev. 1993; 12:303–324. [PubMed: 8281615]

35. LaViolette, PS.; Daun, M.; Cohen, AD.; Connelly, J.; Schmainda, KM. Optimizing repeatability of independent component analysis applied to dynamic susceptibility contrast MRI in 68 brain tumor patients with five repeated scans; Proceedings of the 21st Annual Meeting of ISMRM Salt Lake City; 2013;

36. LaViolette, PS.; Daun, M.; Prah, M.; Jafari-Khouzani, K.; Polaskova, P.; Gerstner, ER.; Stufflebeam, SM.; Schmainda, KM. Repeatability of Independent Component Analysis applied to

Dynamic Susceptibility Contrast MRI in Newly Diagnosed Brain Tumor Patients with Two Baseline Imaging Scans; Proceedings of the 21st Annual Meeting of ISMRM Salt Lake City; 2013;

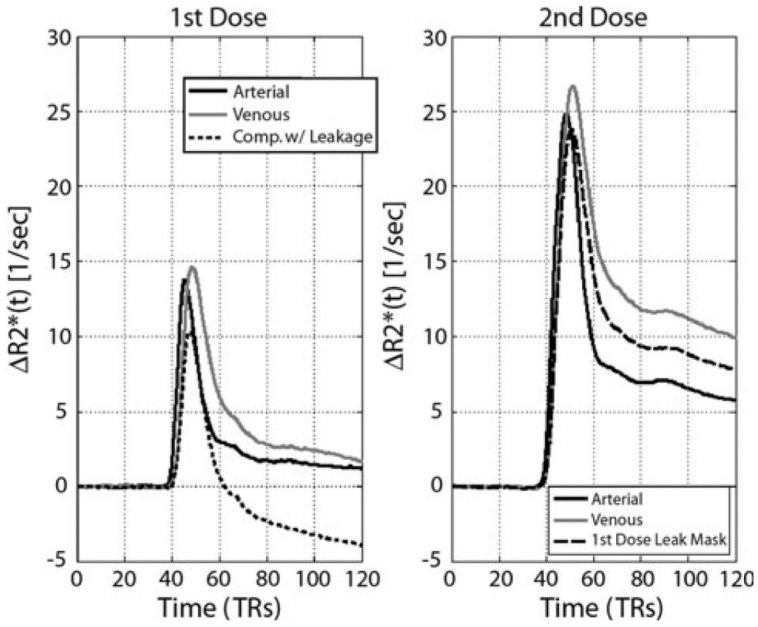

Fig. 1.

ΔR2* time-series for each of the components averaged across patients for each dose. For the first dose (*left*), time-series are shown for the arterial, venous, and the leakage-affected third component. The time-series for the second dose shown include arterial, venous, and the average signal within a mask defined by the leakage-affected first dose component

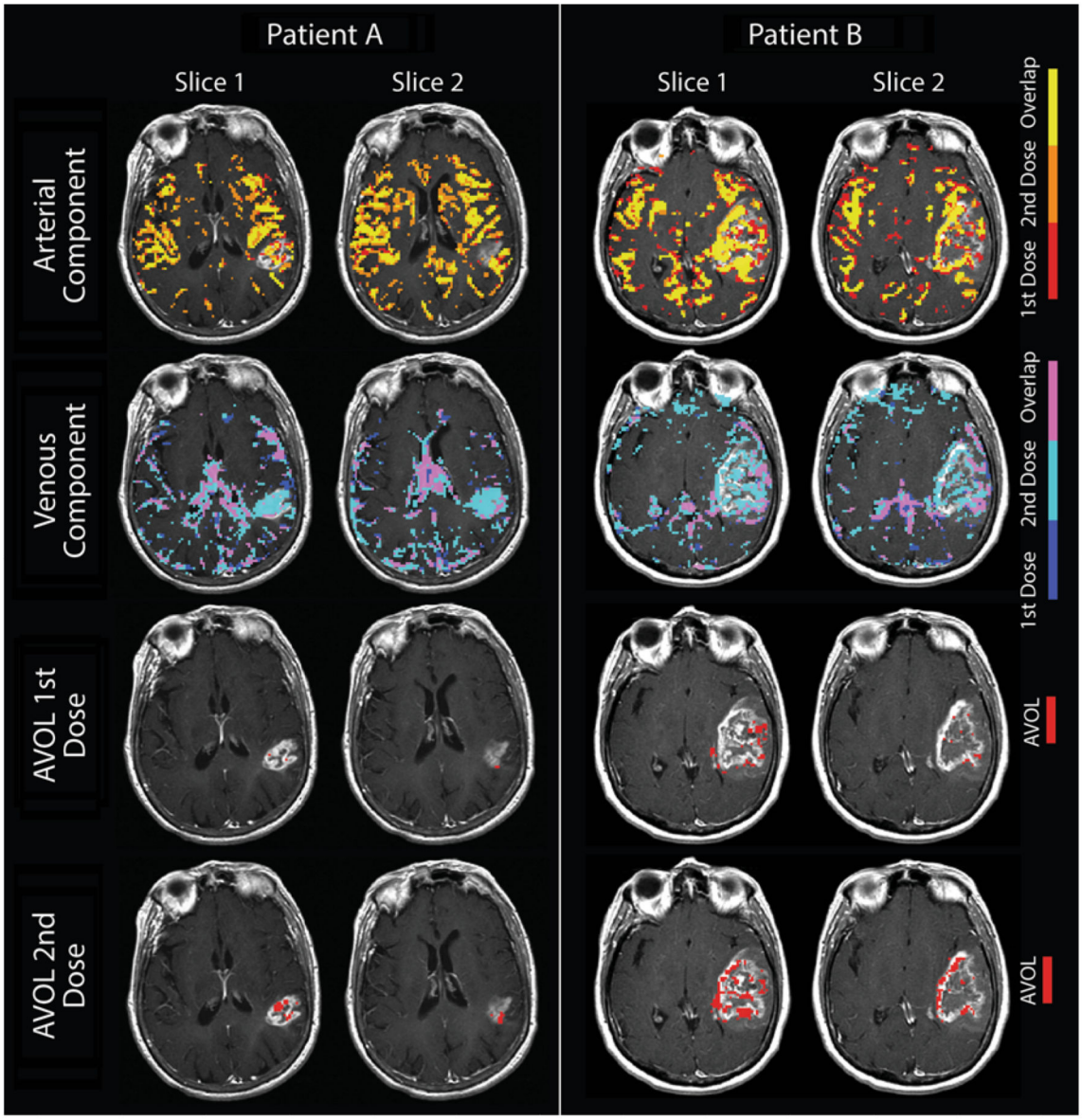

Fig. 2.

Demonstration of component separation of DSC MRI by independent component analysis and the resulting overlap between the two contrast doses. Component maps are overlaid on T1+ contrast imaging from two representative patients. The *first* and *second rows* show the overlap of the arterial and venous components for each dose. Note the dominance of the second dose's venous component within the enhancing tumor (teal). The *bottom two rows* show the AVOL within enhancement resulting from the first and second dose DSC acquisitions. Note the percentage of enhancement classified as AVOL is markedly increased for the second dose

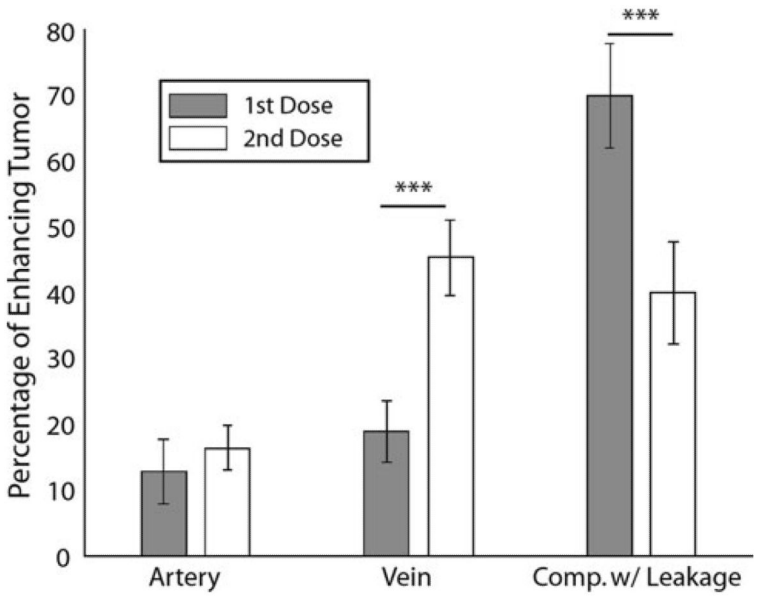

Fig. 3.

Component percentage within enhancing tumor versus dose. The percentage of enhancing tumor classified as venous is significantly greater during the second dose, while the leakage percentage is significantly greater during the first dose. (*** $p < 0.001$) This indicates that a second dose decreases the proportion of enhancing voxels misclassified as non-venous

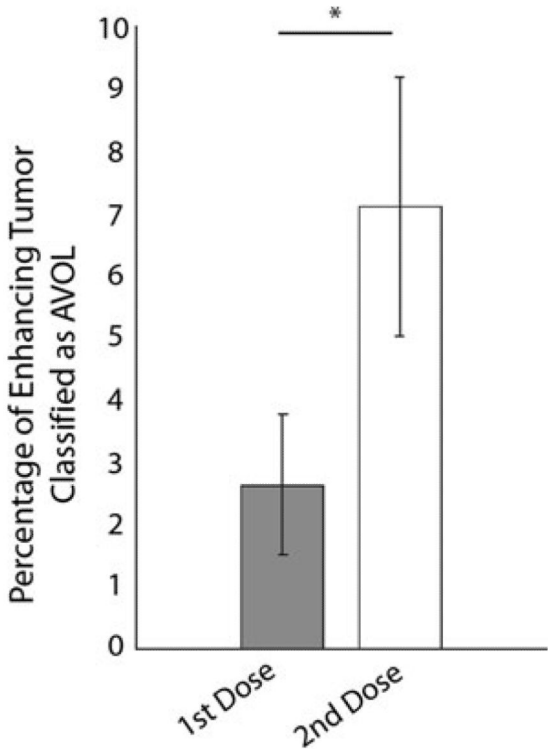

Fig. 4.
Effect of contrast agent leakage on AVOL within enhancement. (* $p < 0.01$)

Table 1

Patient demographics and diagnosis

Subject no	Sex	Age	WHO grade	Histopathologic diagnosis
1	M	69	IV	Glioblastoma multiforme
2	F	35	IV	Residual glioblastoma multiforme
3	F	48	IV	Glioblastoma multiforme
4	F	21	III	Malignant glioneural tumor
5	F	56	III	Recurrent anaplastic oligodendroglial/ astrocytoma
6	F	76	IV	Glioblastoma multiforme
7	M	40	III	Anaplastic oligodendroglioma
8	M	52	III	Recurrent malignant astrocytoma/ oligodendroglial
9	F	44	III	Glioblastoma multiforme
10	F	61	IV	Glioblastoma multiforme